Journal of Thermal Analysis and Calorimetry, Vol. 89 (2007) 3, 761–766

QUANTIFICATION OF DRUG AMORPHOUS FRACTION BY DSC

Giovanna Bruni[1*], *C. Milanese*[1], *G. Bellazzi*[1], *V. Berbenni*[1], *P. Cofrancesco*[1], *A. Marini*[1] *and M. Villa*[2]

[1]C.S.G.I., Dipartimento di Chimica Fisica "M. Rolla", Università degli Studi di Pavia, Viale Taramelli 16, 27100 Pavia, Italy
[2]C.S.G.I., Dipartimento di Progettazione e Tecnologie, Università degli Studi di Bergamo, Viale Marconi 5, 24044 Dalmine, Italy

The processes of production of drugs and dosage forms in the solid state often cause unwanted transformation of portions of the substances into amorphous state, with significant changes of properties such as stability and bio-availability. When this amorphous fraction is of the order of a few percent, it usually goes unnoticed, but it should be accurately determined within a quality control system. In this work, we consider a model drug, perphenazine, where partial amorphisation may be induced by standard mechanical treatments.

We show that Differential Scanning Calorimetry (DSC) leads to consistent estimations of the amorphous fractions induced by the treatment. Furthermore, DSC also yields the expected amounts of amorphous perphenazine when analysing known mixtures of perfectly crystalline samples (untreated) and partially amorphous samples (treated). We show that even amorphous fractions of the order of 1% are accurately estimated by our method.

Keywords: *amorphous state, ball-milling, crystalline solids, drugs, DSC, mechanical activation, thermal methods*

Introduction

During the technological processes of dosage forms production, alteration of the drug original crystal order takes place as a consequence of changing temperature, humidity and pressure of the sample. In particular, milling usually reduces the crystal order by producing lattice defects which propagate from the surface to the bulk crystal [1–8].

Among the phase transitions, amorphisation is one of the most common. Amorphous forms of drugs often exhibit desirable physical-chemical properties [9], such as higher dissolution rate and better solubility, relative to their crystalline counterparts [10, 11]. Unfortunately, the thermodynamically unstable nature of amorphous solids eventually leads to more stable forms, but the kinetics of the process is most often unpredictable and dosage forms with partially unknown properties may be obtained. Whether we want a (partially) amorphous drug or not, it is always important to have the possibility of quantitatively determining the relative mass of the amorphous phase, particularly when it is a small fraction (few %), either in the active ingredient or in the dosage form.

A range of techniques have been applied to determine the relative amount of an amorphous phase: X-ray diffraction, water vapour sorption, DSC and microcalorimetry [12–17], FT-Raman spectroscopy [18], ^{13}C CPMAS-NMR (Cross Polarization Magic Angle Spinning) [19]. Water sorption has proved to be the most sensitive technique while it is usually held that X-ray diffraction and DSC are unable to detect an amorphous phase if it is less than 10% of the sample mass.

In this work, we develop an experimental model to assess sensitivity, accuracy, and detection limit of the DSC technique in quantifying the amorphous phase. We first make a preliminary study of the extent to which mechanical treatments cause amorphisation of perphenazine, 2-chloro-10-[3-[1-(2-hydroxyethyl)-4-piperazinyl]propyl]phenolthiazine, the substance we choose as model drug.

Perphenazine is a phenothiazine derivative belonging to the group of piperazines, a class of neuroleptic drugs used in the treatment of psychosis and schizophrenia.

Experimental

Materials

The samples have all been obtained from a single commercial batch of perphenazine (SIGMA, batch no.: 064H0447) with a stated purity better than 99.9%. The measurements have been performed on the original samples (**AR**, as received) and on samples treated and prepared as described below.

* Author for correspondence: bruni@matsci.unipv.it

1388–6150/$20.00

Akadémiai Kiadó, Budapest, Hungary
Springer, Dordrecht, The Netherlands

We placed a load of about 500 mg of **AR** perphenazine in a planetary mill, Pulverisette 7 (Fritsch) for variable times, at room temperature. Initially, the same ball milling procedure was carried out in agate and in stainless steel jars (3 balls with 10 mm diameter for the agate jar; 10 balls with 3 mm diameters for the stainless steel jar) to check if the milling medium had any effect. The rotation of the main plate was 500 rpm. The samples were milled for 2, 12 and 48 h. The milled samples will be indicated with $\mathbf{BM_x}$, where the subscript is milling time in hours.

Mixtures of weighted **AR** and $\mathbf{BM_{12}}$ samples (total amount ~200 mg) have been homogenised in a Turbula for 20 min. These physical mixtures will be indicated $\mathbf{PM_y}$, where the subscript indicates the fraction of the **AR** sample in percent.

Methods

Sample micrographs have been taken with a Scanning Electron Microscope (SEM) Cambridge Stereoscan 200 (UK) with gold sputtered samples. X-ray powder diffraction data have been collected with a Bruker D5005 (Bruker Siemens, Germany) system equipped with a θ–θ vertical goniometer and a graphite bent monochromator (CuK_α radiation). Patterns have been recorded in step scan mode (step: 0.015°, counting time: 0.5 s) in the angular range 5–30° 2θ.

The DSC apparatus is a TA2920 calorimeter interfaced with a TA 5000 data system (TA Instruments Inc., USA). Measurements were performed at different heating rates (β=1, 2, 10°C min^{-1}) from 25 to 140°C with samples (4–5 mg) in open aluminum pans under dry nitrogen (45 mL min^{-1}), or wet nitrogen (obtained by bubbling N_2 through water at r.t.). Temperature and enthalpy calibrations were performed with pure (>99.999%) indium samples. DSC measurements were combined with annealing with the following measuring protocol:

- heating (10°C min^{-1}) up to a programmed temperature (70, 75, 80, 85, or 87°C);
- isothermal step of 8–18 h at the programmed temperature;
- cooling (10°C min^{-1}) to room temperature;
- second heating to 140°C.

Thermogravimetric analysis was performed with a TA2950 thermobalance interfaced with a TA 5000 data system. The samples (about 5 mg) were scanned from room temperature to 140°C at 10°C min^{-1} in dry nitrogen (45 mL min^{-1}).

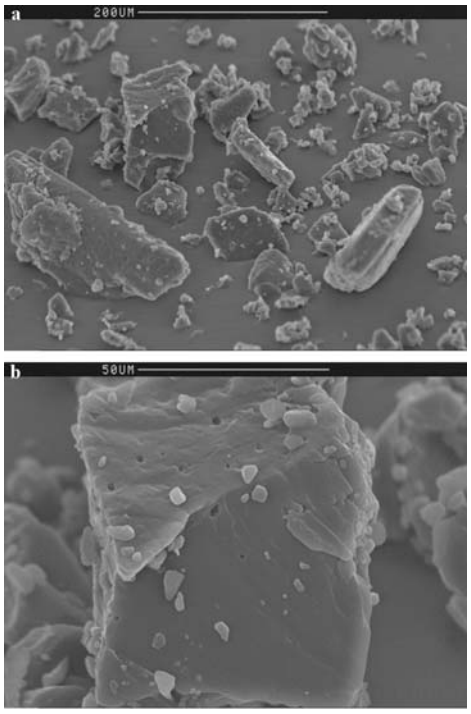

Fig. 1 Micrographs of **AR** perphenazine at different magnifications

Results and discussion

AR sample

SEM pictures of **AR** samples show irregular particles, with size up to about 300 μm (Fig. 1a). Micron size pores and grains are seen over the surface of large grains (Fig. 1b). The diffraction pattern of **AR** samples consists of narrow and sharp peaks, characteristic of a highly crystalline powder (see later). TG runs with **AR** samples do not reveal an appreciable mass change in the entire 25–140°C temperature range. DSC measurements on **AR** samples were carried out at 10°C min^{-1}; each run was repeated three or more times to assess the repro-

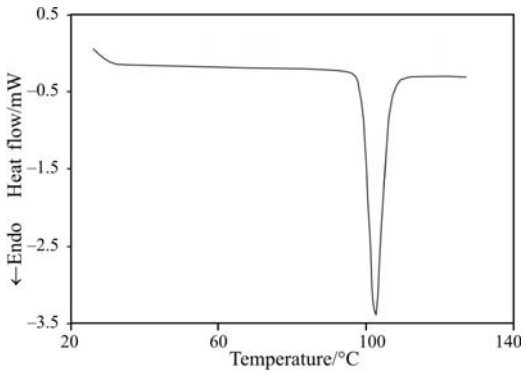

Fig. 2 DSC curve of **AR** sample in dry N_2. Heating rate of 10°C min^{-1}

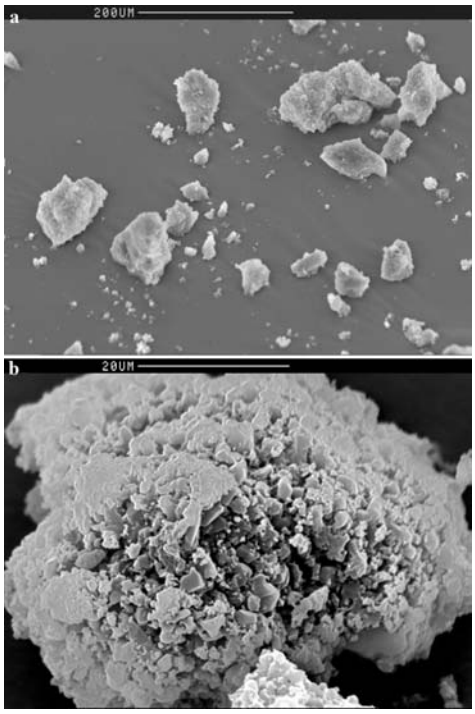

Fig. 3 Micrographs of $\mathbf{BM_2}$ sample at different magnifications

ducibility of these data. The only significant feature in the DSC record of Fig. 2 is the sharp endothermic peak of melting, with an onset temperature T_{on}=98.9±0.1°C and an enthalpy change ΔH= 87.3±1.0 J g^{-1}.

***BM** samples: SEM and X-ray measurements*

The micrographs of $\mathbf{BM_2}$ sample are reported in Fig. 3. As expected, milling causes an important decrease of the grain mean size. Furthermore, the grains now consist of aggregates of micrometric and sub-micrometric particles. There are no appreciable differences between morphologies of samples milled for 2, 12 and 48 h. There is also no significant difference in morphology or thermal behaviour between samples milled with steel or with agate. The sample of Fig. 3 was milled using agate jar and balls, as all the **BM** samples presented in this paper.

The X-ray diffraction patterns of $\mathbf{BM_2}$ and $\mathbf{BM_{48}}$ samples are compared in Fig. 4 with that of the **AR** sample. Milling for 2 h changes heights (smaller), widths at half height (larger), and relative intensities of diffraction peaks, but not their angular positions. Increasing milling times from 2 to 48 h has no apparent effect upon diffraction patterns. We conclude that milling produces no new crystalline phases, and that all structural/morphological changes are achieved in the first two hours of milling.

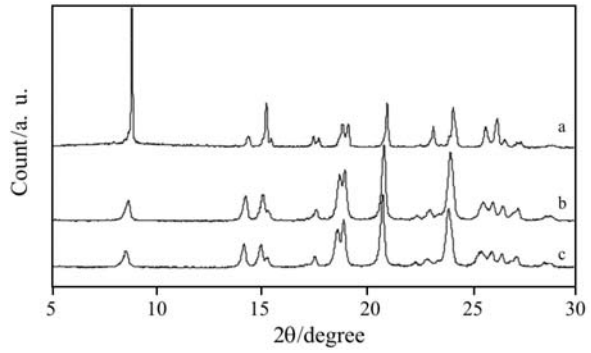

Fig. 4 Diffraction patterns of a – **AR**, b – $\mathbf{BM_2}$ and c – $\mathbf{BM_{48}}$ samples

***BM** samples: DSC measurements*

The DSC recordings carried out at 10°C min^{-1} display a single endothermic peak (melting) quite similar to that of Fig. 2. The enthalpy changes and the onset temperatures measured in dry nitrogen with all **BM** samples are essentially the same within experimental error: ΔH=72.7±2.0 J g^{-1}, T_{on}=92.0±0.3°C. This confirms that milling more than 2 h does not achieve any further effect. On the other hand, both ΔH and T_{on} for ball-milled samples are significantly below the corresponding **AR** values.

Since X-ray data show that no new crystalline phase is formed by milling, we may explain the reduced melting enthalpy of **BM** samples as caused by a partial amorphization of perphenazine. Since the amorphous phase does not melt, and does not contribute to the melting enthalpy, we may estimate the amorphous fraction as the reduction of ΔH divided by the melting enthalpy of **AR**. For the **BM** samples we obtain an average amorphous fraction of 16.7%; the spread of values (from 15% for $\mathbf{BM_{48}}$ to 18% for $\mathbf{BM_{12}}$, with no apparent relationship with the milling time) is compatible with the experimental deviations of the enthalpies.

Another effect of milling is a substantial decrease (~7°C) of the onset temperature of melting. This phenomenon is not an experimental artefact since the experimental conditions were the same: heating rate, dry N_2 atmosphere, sample mass, sample pan. Since it is well known that the heating rate affects in a predictable way the onset temperature, we compared DSC measurements performed at different

Table 1 Mean values and standard deviations of T_{on} and ΔH measured in $\mathbf{BM_{48}}$ samples at different heating rates

β/°C min^{-1}	T_{on}/°C	ΔH/J g^{-1}
1	94.9±0.1	75.8±1.1
2	95.1±0.1	73.6±2.6
10	92.4±0.1	74.1±1.0

rates on **BM$_{48}$** samples. The results are summarised in Table 1.

The enthalpy changes are essentially independent of the heating rate, as it should be. On the other hand, T_{on} is about the same at 1 and 2°C min^{-1} but decreases by 2.5°C when the heating rate is raised to 10°C min^{-1}. This behaviour is contrary to expectation (and to what is observed in **AR** sample), since the thermal lag should increase with increasing heating rate, thus raising the onset temperature.

A qualitative explanation of this anomaly is as follows: during heating, melting begins earlier at the surface of the smallest grains, which are also in better thermal contact with the aluminium pan. In fact, a crucial parameter of DSC is the thermal exchange between sample and heating element through the metal pan. Samples with different morphologies and heat conductivities may have very different time lags; small grains in contact with the pan are expected to display little or no thermal lag.

If the sample is annealed long enough below the onset temperature, small grains have time to merge releasing their surface energy, and avoiding 'pre-melting'. At very 'low' heating rates, all 'small' grains have time to merge, and further reduction of β does not change T_{on}. At very large heating rates, annealing before melting is negligible and thermal lag effects dominate. At some 'intermediate rate', both annealing before melting and thermal lag are not large, and we measure the lowest onset temperature which ideally represents the melting temperature of the original grains.

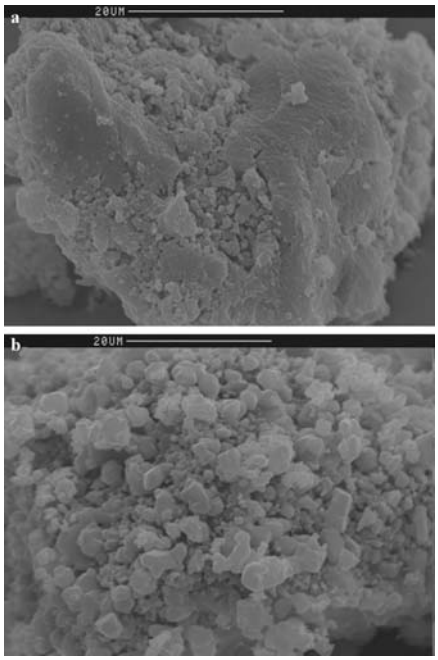

Fig. 5 Micrographs of the a – **BM$_{48}$** and b – **BM$_{48}^{ann}$** samples

Figure 5 compares SEM images of a **BM$_{48}$** and a **BM$_{48}^{ann}$** sample, which was brought to 85°C at 1°C min^{-1} and then cooled to r.t. This figure confirms that **BM$_{48}^{ann}$** sample has a mean particles size larger than the **BM$_{48}$** sample, and that a slow (1°C min^{-1}) scan stopped well before melting is enough to achieve this substantial change of morphology.

We may conclude that the significant decrease of the melting onset temperature is due to the reduced mean particle size achieved by milling.

Annealing and re-crystallization of the amorphous phase

DSC measurements with an annealing step (see the protocol in the experimental section) have been carried out to check if annealing leads to some re-crystallization of the **BM** samples. Essentially, we determine ΔH and T_{on} during a heating run after a hours-long isothermal step below melting, followed by cooling to r.t. The data are summarized in Table 2, together with the pertinent details concerning the annealing treatment. All measurements have been performed on **BM$_{48}$** samples.

Table 2 shows that T_{on} increases with increasing annealing temperature and time, in agreement with our qualitative argument. Figure 6 compares micrographs of a **BM$_{48}$** sample before and after annealing (12 h at 85°C under dry nitrogen, sample code **BM$_{48}^{iso}$**) and shows that the effect of the annealing is an increase of the mean particle size even larger than that demonstrated in Fig. 5.

We call attention to the melting enthalpies of Table 2: they are similar for all annealed samples, and intermediate between ΔH of not-annealed **BM**s and that of **AR**. This fact implies that partial re-crystallization takes place during annealing. Table 2 shows that 8 h annealing at 70°C under dry nitrogen produces the same re-crystallization effect of an isothermal treatment of 18 h at 87°C under wet nitrogen. In other words, the amorphous phase

Table 2 Temperature (T_{iso}) and time (t_{iso}) of annealing, atmosphere, onset temperature (T_{on}) and melting enthalpy (ΔH) of annealed **BM$_{48}$** samples

T_{iso}/ °C	t_{iso}/ h	Atmosphere	T_{on}/ °C	ΔH/ J g^{-1}
70	8	N_2	93.8±0.2	79.6±1.8
75	12	N_2	94.1±0.2	78.8±1.9
80	12	N_2	95.8±0.2	80.7±2.1
85	18	N_2	96.8±0.2	83.2±1.6
85	18	Wet N_2	96.5±0.2	81.6±1.9
87	18	Wet N_2	96.8±0.2	78.6±2.0
		Mean value		80.4±1.8

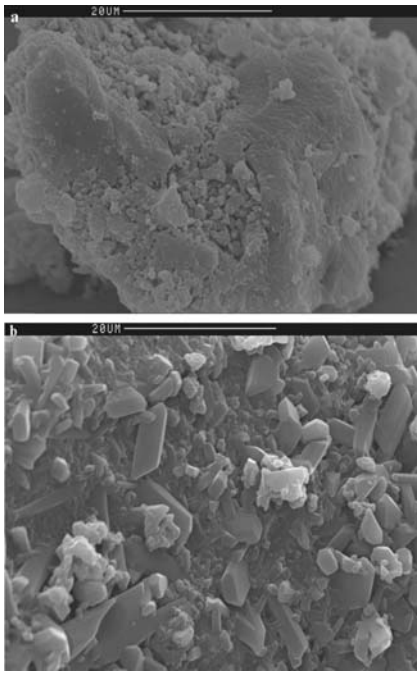

Fig. 6 Micrographs of the a – $\mathbf{BM_{48}}$ and b – $\mathbf{BM_{48}^{iso}}$ samples

obtained by milling seems to be quite stable, and full crystallization may be very difficult to achieve.

By comparing the melting enthalpies of the **AR** and **BM** samples before and after annealing, we obtain that the annealing causes crystallization of about 50% of the amorphous phase which was originally present in the **BM** samples.

*Mixtures of **AR** and **BM** samples*

A simple way to obtain samples with different amounts of amorphous/crystalline phase is to mix known amounts of **AR** sample (that we assume to be perfectly crystalline) and **BM** sample (partially amorphous and with a known share of amorphous phase). DSC measurements with these mixtures allow to determine the accuracy of the DSC method and its capability of detecting small amorphous fractions.

Figure 7 shows some DSC traces obtained in different mixtures while Table 3 reports the corresponding onset temperatures. Details of the melting peaks and behaviour of the onset temperatures depend

Table 3 Onset temperature for mixtures

Mixture	T_{on}/°C
$\mathbf{PM_{10}}$	91.5±0.3
$\mathbf{PM_{20}}$	95.9±0.1
$\mathbf{PM_{50}}$	97.4±0.2
$\mathbf{PM_{80}}$	98.3±0.1
$\mathbf{PM_{90}}$	99.0±0.4
$\mathbf{PM_{95}}$	98.9±0.3

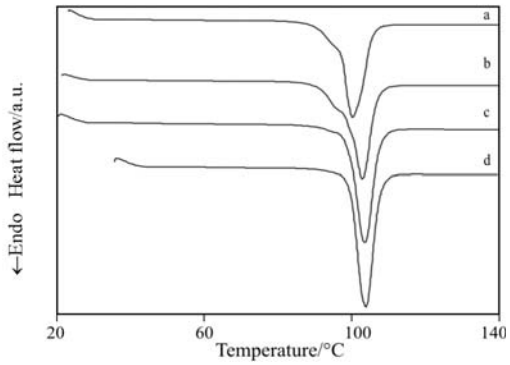

Fig. 7 DSC curves of the mixtures of **AR** and $\mathbf{BM_{12}}$ samples. a – $\mathbf{PM_{20}}$, b – $\mathbf{PM_{50}}$, c – $\mathbf{PM_{80}}$, d – $\mathbf{PM_{95}}$

as expected on composition. In the mixtures with a high **BM** component, the melting peak has a low-temperature shoulder (see in Fig. 7 the $\mathbf{PM_{20}}$ and $\mathbf{PM_{50}}$ mixtures) and the T_{on} values are, as expected, lower for $\mathbf{PM_{20}}$ and higher for $\mathbf{PM_{50}}$ (Table 3). With decreasing the relative content of **BM** component (i.e. the relative content of the amorphous phase), T_{on} increases and the low temperature shoulder, barely visible in $\mathbf{PM_{80}}$, has disappeared in $\mathbf{PM_{95}}$.

The error analysis may be performed by comparing, for each mixture, the expected (ΔH_{exp}) and measured (ΔH_{meas}) values of the melting enthalpies. The expected values are calculated as weighted mean (the composition as mass coefficient) of the melting enthalpies recorded for the single components of the mixture (**AR** and **BM** samples).

The ΔH_{exp} and ΔH_{meas} values obtained for the mixtures are reported, together with the mixture composition, in the first columns of Table 4. Again, the standard deviations (not the standard error!) reported for the ΔH_{meas} values have been obtained from at least three independent measurements. The uncertainties of ΔH_{exp} have been assumed, for simplicity, equal to the highest standard deviation of the two components.

The measured enthalpy changes agree quite well with the expected ones, suggesting that our model is

Table 4 ΔH_{exp} and ΔH_{meas} values and percentage amounts of expected (Q_{exp}) and experimental (Q_{meas}) amorphous phase for mixtures

Mixture	ΔH_{exp}/ J g^{-1}	ΔH_{meas}/ J g^{-1}	Q_{exp}/ mass%	Q_{meas}/ mass%
$\mathbf{PM_{10}}$	73.1±1.5	74.3±0.7	16.3	14.9
$\mathbf{PM_{20}}$	74.7±1.5	75.1±2.1	14.4	13.9
$\mathbf{PM_{50}}$	79.4±1.5	79.8±1.9	9.0	8.6
$\mathbf{PM_{80}}$	84.1±1.5	82.6±0.8	3.7	5.4
$\mathbf{PM_{90}}$	85.7±1.5	84.4±0.3	1.8	3.3
$\mathbf{PM_{95}}$	86.5±1.5	86.3±0.2	0.9	1.1

based upon a set of consistent hypotheses. The experimental (Q_{meas}) and expected (Q_{exp}) fractions of amorphous phase deduced from the mean enthalpy values are reported in the last columns of Table 4. This table just shows that the method may reliably estimate even a 1% amorphous fraction. This could seem strange, since our precision, i.e. deviations of enthalpy changes over all our samples, correspond to about 1.5%. However, with repeated (averaged) data, the detection limit is certainly below 1%.

Further remarks about the detection limit of the amorphous phase are now made with reference to **PM_{95}** mixture, with an expected content of amorphous phase of 0.9%. We believe that the good agreement with the measured value of 1.1% is not so much due to good luck, but to the fact that we systematically used mean ΔH values averaged over several data, and with an uncertainty about two times smaller than the standard deviation.

Conclusions

Partial amorphization of crystalline samples of perphenazine has been induced by high-energy milling. The maximum level of amorphisation (~17%) is achieved with just two hours milling; longer treatments do not change the properties of the sample. The amorphous phase is kinetically stable; about half of it re-crystallizes during hours-long annealing.

The fraction of amorphous phase obtained by mechanical activation can be reliably evaluated by differential scanning calorimetry. By comparing the expected content of amorphous phase in mixtures of as received sample (assumed to be pure crystals) and ball milled samples (with known content of amorphous phase) we show that DSC may, in principle, detect also 1% of the amorphous form.

References

1 A. Marini, V. Berbenni, G. Bruni, P. Cofrancesco, F. Giordano and M. Villa, Curr. Med. Chem., Anti-infective Agents, 2 (2003) 303.
2 G. G. Zhang, D. Law, E. A. Schmitt and Y. Qiu, Adv. Drug Del. Rev., 56 (2004) 371.
3 J. F. Willart, A. De Gusseme, S. Hemon, G. Odou, F. Danede and M. Descamps, Solid State Commun., 119 (2001) 501.
4 E.Yonemochi, S. Kitahara, S. Maeda, S. Yamamura, T. Oguchi and K. Yamamoto, Eur. J. Pharm. Sci., 7 (1999) 331.
5 L. R. Hilden and K. R. Morris, J. Pharm. Sci., 93 (2004) 3.
6 M. K. Gupta, A. Vanwert and R. H. Bogner, J. Pharm. Sci., 92 (2003) 536.
7 A. A. Elamin, C. Ahlneck, G. Alderborn and C. Nyström, Int. J. Pharm., 111 (1994) 159.
8 L. Mackin, S. Sartnurak, I. Thomas and S. Moore, Int. J. Pharm., 231 (2002) 213.
9 D. Q. M. Craig, P. G. Royall, V. L. Kett and M. L. Hopton, Int. J. Pharm., 179 (1999) 179.
10 L. Yu, Adv. Drug Del. Rev., 48 (2001) 27.
11 B. C. Hancock and M. Parks, Pharm. Res., 17 (2000) 397.
12 A. Saleki-Gerhardt, C. Ahlneck and G. Zografi, Int. J. Pharm., 101 (1994) 237.
13 K. Kawakami, T. Numa and Y. Ida, J. Pharm. Sci., 91 (2002) 417.
14 H. Ahmed, G. Buckton and D. A. Rawlins, Int. J. Pharm., 130 (1996) 195.
15 R. Chadha, N. Kashid and D. V. S. Jain, J. Therm. Anal. Cal., 81 (2005) 277.
16 M. Lappalainen and I. Pitkanen, J. Therm. Anal Cal., 84 (2006) 345.
17 R. C. Mashru, V. B. Sutariya, M. G. Sankalia and P. Yagnakumar, J. Therm. Anal. Cal., 82 (2005) 167.
18 L. S. Taylor and G. Zografi, Pharm. Res., 15 (1998) 755.
19 R. Lefort, A. De Gusseme, J. F. Willart, F. Danède and M. Descamps, Int. J. Pharm., 280 (2004) 209.

DOI: 10.1007/s10973-006-7943-1